9th International Conference on Information and Knowledge Technology (IKT 2017)
October 18 & 19, 2017, Amirkabir University of Technology

A New Statistical Detector for CT-Based Multiplicative Image Watermarking Using the t Location-Scale Distribution

Sadegh Etemad
Dep. of Computer Engineering and Info.Technology
Amirkabir University of Technology
Tehran, Iran
etemad.sadegh@aut.ac.ir

Maryam Amirmazlaghani
Dep. of Computer Engineering and Info.Technology
Amirkabir University of Technology
Tehran, Iran
mazlaghani@aut.ac.ir

Abstract— **In this study, a new statistical multiplicative watermark detector in contourlet domain is presented. The contourlet coefficients of images are highly non-Gaussian and a proper distribution to model the statistics of the contourlet coefficients is a heavy-tail Probability Distribution Function (PDF). In this study, a multiplicative watermarking scheme is proposed in the contourlet domain using t location-scale distribution (tLS). Afterward, we used the likelihood ratio decision rule and tLS distribution to design an optimal multiplicative watermark detector. The detector showed higher efficiency than other watermarking schemes in the literature, based on the experimental results, and its robustness against different attacks was verified.**

Keywords- t Location-Scale Distribution; Contourlet transform; Multiplicative Image Watermarking; Maximum Likelihood.

I. INTRODUCTION

In recent years, due to increasing digital media on the internet, copyright protection turns into an essential problem. One of the most popular approaches for the deal with this problem is digital watermarking. Digital watermarking has been proposed as a technology for copyright protection and content authentication. At the first step of digital watermarking, the secondary data (watermark) embedded into digital media such as image, audio, video, and text. Afterward, in the second step, the embedded watermark extract. The first and second steps of digital watermarking are called watermark embedding and watermark extraction, respectively. Some applications of digital watermarking include broadcast monitoring, tamper proofing, fingerprinting, content archiving, copyright protection and secret communication. In this research, use of watermark detection for copyright protection was examined.

In the literature, digital watermarking methods categorized in different ways based on embedding domain: spatial [1] or frequency [2], the embedding methods: spread spectrum [3] or quantization based [4], and the extraction methods: detection or decoding. Since frequency domain technique more robust under different types of attacks, it's favored to the spatial domain. Image watermarking has been studied extensively in the transform domain such as Discrete Cosine Transform (DCT) [5,6], Discrete Fourier Transform (DFT) [7], Discrete Wavelet Transform (DWT) [8,9], Contourlet Transform (CT) [10,11] and Ridgelet Transform [12]. At the early stage of the studies, some of transform domain watermarking methods implemented in the DCT, DFT. Later, the DWT-based watermarking methods were present. Next, [13] demonstrates the outperformance of the contourlet-domain algorithms against the attacks compared with other frequency-domain watermarking schemes. There are some advances in contourlet domain over other directional representations such as wavelet. The contourlet transform able to have several directions while obtaining nearly critical sampling. Also for computationally efficient implementation, it uses the iterated filter banks. Hence, in this work, we focus on image watermarking in contourlet domain.

Spread spectrum embedding methods use two basic embedding techniques: additive and multiplicative. In [10], we applied additive embedding rule for the watermarking scheme. But since the multiplicative embedding method can model the Human Visual System (HVS) preferred to additive embedding methods. Also, the multiplicative watermarks are image content dependent [14]. So, in this study, we improved [10] by using multiplicative embedding in our watermarking scheme.

According to [15], the contourlet coefficients have large peaks and are highly non-Gaussian; they also have heavier tails compared to a Gaussian probability density function, so, we can't use correlation detector. Previous works used various PDFs as the prior distribution for contourlet coefficients. Some of the distribution that used for modeling the contourlet coefficients include generalized Gaussian [16], Normal inverse Gaussian(NIG) [17], Alpha-stable [18] and Bessel k Form (BKF) [11] distribution.

In this work, we propose a new statistical multiplicative contourlet domain watermark detector using t location-scale distribution. The detector showed higher efficiency than other watermarking schemes in the literature, based on the experimental result, and its robustness against different attacks was verified. We observed that the watermark detection performance has enhanced as compared to other detectors such as additive tLS, multiplicative BKF, and GG detectors.

The rest of the paper is as follows. Modeling of contourlet coefficients is presented in section 2. Section 3 presents the multiplicative watermarking method in the contourlet domain.

978-1-5386-2547-7/17/$31.00 ©2017 IEEE

Performance of tLS detector is assessed in section 4. Conclusions are finally presented in section 5.

II. STATISTICAL MODELING

In the first part of this section, we analyzed the location-scale family distributions and reviewed the tLS distribution then in the second part, contourlet coefficient modeling was examined using tLS distribution.

A. t location-Scale Distribution (tLS)

A x as a random variable (RV) follows a student's t distribution [19]

$$f(x;v)=\frac{\Gamma(\frac{v+1}{2})}{\sqrt{v\pi}\Gamma(\frac{v}{2})}(1+\frac{x^2}{v})^{-(\frac{v+1}{2})} \quad (1)$$

Parameter $v>0$ determines the degree of freedom and Γ denotes the gamma function, which is defined as

$$\Gamma(a)=\int_0^\infty x^{a-1}e^{-x}dx \quad (2)$$

Where $a>0$.

Student's t distribution can be generalized to a tLS by applying the linear transformation $Y=\mu+\sigma X$. Through application of a linear transformation, we can easily shift the center of the distribution and affect the divergence from its mean.

So, if $X \sim Student's(v)$ then Y follows the t location scale distribution (or non-standard Student's t distribution) with the parameters μ,σ,v. The PDF of t location-scale distribution is

$$f\_tls(y;\mu,\sigma,v)=\frac{\Gamma(\frac{v+1}{2})}{\sigma\sqrt{v\pi}\Gamma(\frac{v}{2})}(1+\frac{1}{v}(\frac{y-\mu}{\sigma})^2)^{-(\frac{v+1}{2})} \quad (3)$$

where $-\infty<\mu<+\infty$, $\sigma>0$ and $v>0$ are respectively the parameters of location, scale and shape. The maximum likelihood estimator can be used to determine parameters of location, scale, and shape [19].

B. Contourlet Coefficient Modeling with tLS

In [13], Do and Vetterli introduced contourlet transform for obtaining sparse expansions. In this transform, Laplacian pyramid (LP) is applied to the original image to reach multiscale decomposition when the coarse image is iteratively subsampled and each residual image is fed into the directional filter bank (DFB) to obtain directional information. Fig.1 shows the results of applying contourlet transform on the "Barbara" image. At first, the image disintegrated in two pyramidal levels. Next, the DFB applied on the image to obtain four and eight directional subbands.

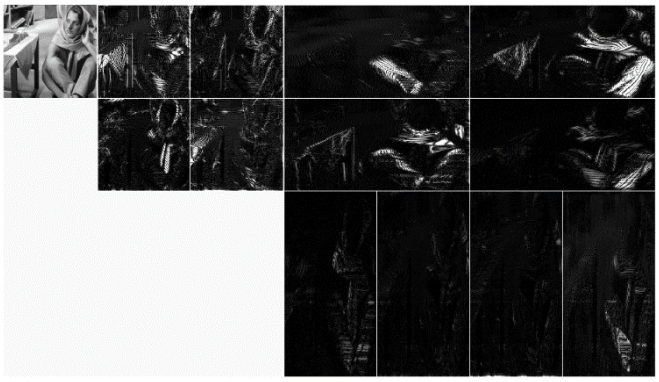

Figure 1. Barbara image contourlet coefficients for two finest scale.

Since the contourlet coefficients have heavy-tailed, non-Gaussian distributions, a proper distribution is needed for modeling contourlet coefficients, which present large peaks and heavier tails compared to the Gaussian PDF. In this research, tLS distribution is used to model the contourlet coefficients. Fig.2 represents the log-scale histogram of contourlet coefficients and the log-scale pdf of the best fitted tLS, student's t and generalized Gaussian(GG) distributions for Barbara image (8th and 9th subband at fourth level of pyramidal decomposition). This figure demonstrates that the tLS distribution is well fitted while student's t distribution fails in modeling contourlet coefficients. Also, in comparison with generalized Gaussian distribution, tLS distribution has better performance for modeling the contourlet coefficients.

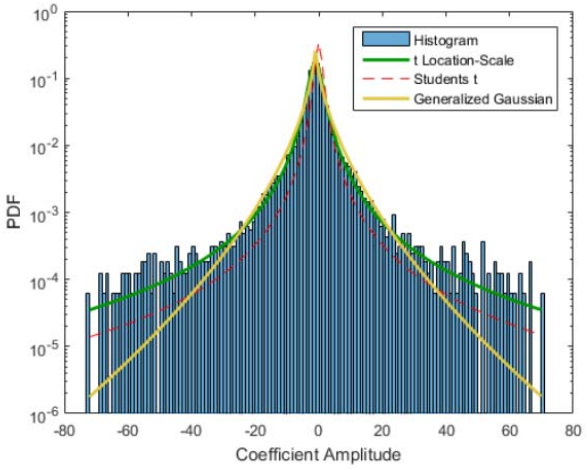

(a)

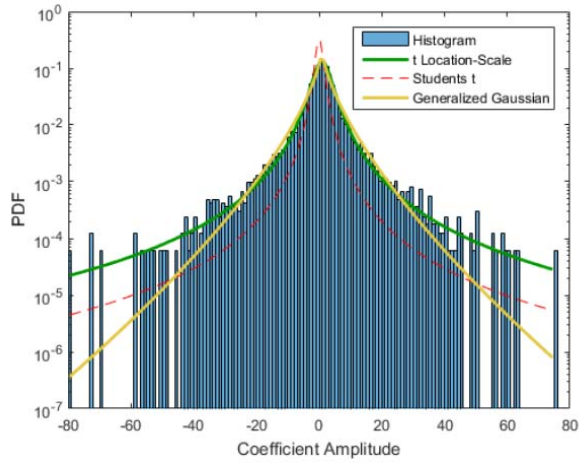

(b)

Figure 2. The log-scale histogram of contourlet coefficients for Barbara image at (a) 8th and (b) 9th subband in the fourth level of pyramidal decomposition and the best fitted t location scale, student's t and generalized Gaussian distributions.

Similar results were obtained on different subbands for other images.

III. WATERMARKING SCHEME

Watermark embedding and detection comprise a watermarking scheme. So, in this section, we described them.

A. Watermark Embedding

In the watermark embedding step, we use a contourlet domain multiplicative spread spectrum embedding scheme. For this purpose, first, we applied the contourlet transform with the fourth level of pyramidal decomposition and sixteen directions of directional filter banks to the original images. So, for each image, the contourlet coefficients of the directional subband, $X=[x_1,x_2,...,x_N]$, is calculated. Then, to embed the watermark bits into the directional subband coefficients, we select the subband that has maximum energy. The energy of each directional subband calculated as follows:

$$E_{j,k}=\frac{1}{A\times B}\sum_{m=1}^{M}\sum_{n=1}^{N}\left(X_{j,k}^{l_j}(m,n)\right)^2 \qquad (4)$$

Where $X_{j,k}^{l_j}$ refers to the subband image at j-th decomposition level and k-th bandpass directional image, decomposed by an l_j-th level DFB. $A\times B$ shows subband size, and $E_{j,k}$ is the subband energy at j-th decomposition level and k-th bandpass. Later, we use multiplicative embedding rule for embedding watermark in the selected directional subband as following

$$y_i=x_i\times(1+\alpha w_i) \qquad (5)$$

Where $W=[w_1,w_2,...,w_N]$ is the watermark sequence, α is the embedding power, $Y=[y_1,y_2,...,y_N]$ refers to watermarked contourlet coefficients. W represents the bipolar watermark with similar probability (-1 and 1). According to watermark to document ratio (WDR) value, the embedding power (α) value for each image is calculated.

Now, to investigate the imperceptibility of embedding step, we have plotted Fig. 3. In the first row of Fig.3 the original images (Barbara, Airplane, Boat and Lena) are presented. The corresponding watermarked images and the difference between them have been shown in middle and bottom rows of Fig.2, respectively. The peak signal-to-noise ratio (PSNR) and mean square error (MSE) are common indices for analyzing the invisibility of embedding. The values of the MSE, PSNR and α show in Table I.

Figure 3. Original, watermarked and difference images respectively. the Barbara, Airplane, Boat and Lena with size 512× 512 are test images (WDR=-55).

It can be seen from Fig.3 and Table I that the images are indistinguishable with high PSNR values. Hence, we achieved the imperceptibility of the embedded watermark at the embedding step.

TABLE I. THE VALUE OF MSE , PSNR AND α (WDR=-55)

Image	PSNR	MSE	α
Barbara	53.94	0.2623	0.0625
Airplane	67.89	0.0105	0.0279
Boat	67.83	0.0107	0.0282
Lena	76.72	0.0013	0.0168

B. Watermark Detection

Since, the application of paper is copyright protection, we should verify the existence of a known watermark. In this section, to detect the watermark in the contourlet subband coefficients, we develop an optimum detector based on the tLS PDF. The watermark detection can be represented as binary hypothesis test:

$$H_0 : y_i = x_i \quad \text{i=1,2,...,N} \tag{6}$$

$$H_1 : y_i = x_i \times (1+\alpha w_i) \quad \text{i=1,2,...,N} \tag{7}$$

H_0 and H_1 represent respectively the null (the watermark does not exist) and alternative (the watermark exists) hypotheses.

We assume the original image coefficients (x_i) to be independent and identically distributed (i.i.d) and follow a tLS distribution with the parameters (v, μ, σ) as defined in (3). So, due to (6) and (7), the distribution of the contourlet coefficients under null and alternative hypothesis can be computed as:

$$H_0 : P(y \mid H_0) = \prod_{i=1}^{N} f\_tls(y_i, \mu, \sigma, v) \tag{8}$$

$$H_1 : P(y \mid H_1) = \prod_{i=1}^{N} f\_tls(y_i, \mu \times (1+\alpha w), \sigma \times (1+\alpha w), v) \tag{9}$$

f_tls indicates the tLS distribution as determined in (3). the likelihood ratio test (LRT) was applied, considering its efficacy based on the Neyman-Pearson criterion. So, we employ the LRT for a subband as:

$$\Lambda(y) = \frac{P(y \mid H_1)}{P(y \mid H_0)} \underset{H_0}{\overset{H_1}{\gtrless}} \eta \tag{10}$$

Where η denotes threshold that is computed using Neyman-Pearson criteria. By integrating (8) and (9) in (10) and using (2), we have

$$\Lambda(y) = \prod_{i=1}^{N} \left((1+\alpha w_i)^{-1} \left[\frac{v + \left(\frac{y_i - (1+\alpha w_i)\mu}{(1+\alpha w_i)\sigma} \right)^2}{v + \left(\frac{y_i - \mu}{\sigma} \right)^2} \right]^{-\left(\frac{v+1}{2}\right)} \right) \tag{11}$$

To mathematical simplification, the log-likelihood ratio test (LLRT) instead of LRT was used. So; we have

$$LLRT(y) = \sum_{i=1}^{N} \left[-\ln(1+\alpha w_i) + \left(\frac{v+1}{2}\right) \ln\left(v + \left(\frac{y_i - \mu}{\sigma} \right)^2 \right) - \left(\frac{v+1}{2}\right) \ln\left(v + \left(\frac{y_i - (1+\alpha w_i)\mu}{(1+\alpha w_i)\sigma} \right)^2 \right) \right] \tag{12}$$

Equation (12) is Maximum Likelihood(ML) detector that we proposed.

IV. Simulation Results

In this section, we study the performance of tLS watermark detector on many images [20]. Since we have limited space for reporting the results, we only publish the results of four grayscale images, namely, *Barbara, Airplane, Boat, and Lena* (512 × 512).

In the following, we first examine the performance of the t location-scale detector without any type of attack and compare it with other contourlet domain detectors such as Bessel K Form (BKF) [11] and Generalized Gaussian (GG) [16] by receiver operating characteristic (ROC) plot. Fig.4 represents the ROCs of the three detectors for images (Barbara, Airplane, Boat and Lena) without any attacks. This figure demonstrates that the higher performance of our detector versus other detectors.

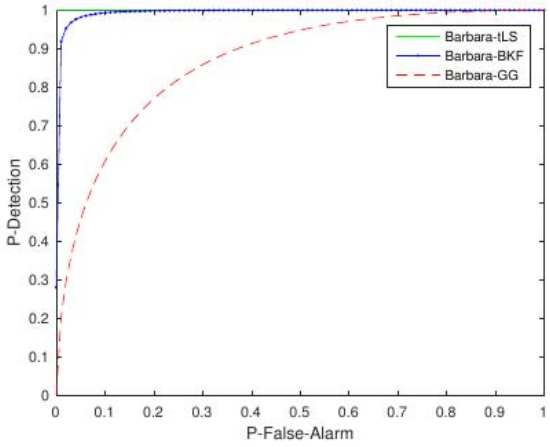

(a)

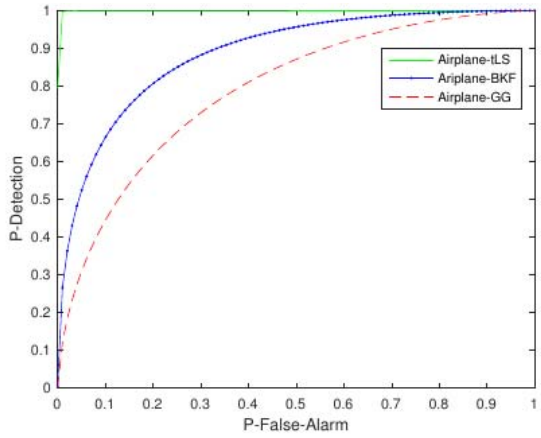

(b)

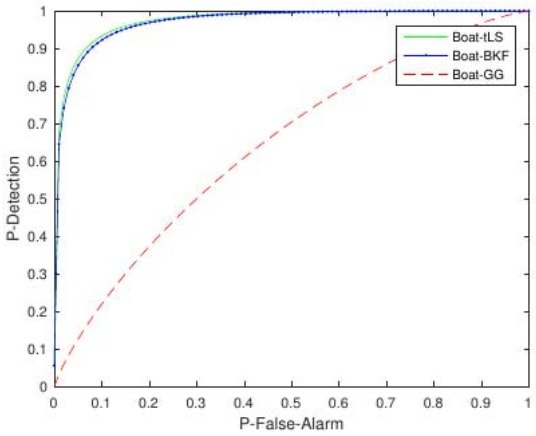

(c)

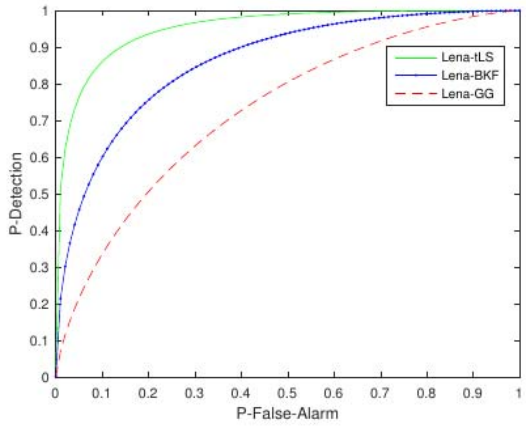

(d)

Figure 4. ROC curve using tLS, BKF and GG based detectors without any attacks on test images (a)Barbara, (b)Airplane, (c)Boat and (d)Lena (WDR=-55 db).

Then, we examine the performance of the BKF, GG, additive tLS [10] and Multiplicative tLS detectors under different types of attacks by using the area under the ROC (AUROC).

Table II, Table III and Table IV represents the AUROC results of the multiplicative tLS, additive tLS, BKF and GG detectors under JPEG Compression, Gaussian Filter and Rotation Attacks, respectively. In each row of tables, the bold value is the best result. These tables demonstrate the outperformance of the proposed detector.

TABLE II. AUROC VALUES UNDER JPEG COMPRESSION ATTACK (WDR=-55)

Attack type	Images	t-LS	Additive t-LS [10]	BKF [11]	GG [16]
JPEG (QF=45)	Barbara	**0.9998**	0.9660	0.9770	0.9086
	Airplane	**0.9999**	0.8920	0.8699	0.9476
	Boat	**0.9942**	0.8016	0.9550	0.5572
	Lena	**0.9688**	0.7054	0.8278	0.5549

TABLE III. AUROC VALUES UNDER MEDIAN FILTER ATTACK (WDR=-55)

Attack type	Images	t-LS	Additive t-LS [10]	BKF [11]	GG [16]
Median Filtering (4×4)	Barbara	**0.9815**	0.9641	0.7847	0.6776
	Airplane	**0.9999**	0.9933	0.8286	0.8566
	Boat	**0.9982**	0.9029	0.7825	0.7176
	Lena	**0.9973**	0.8826	0.7071	0.8953

TABLE IV. AUROC VALUES UNDER ROTATION ATTACK (WDR=-55)

Attack type	Images	t-LS	Additive t-LS [10]	BKF [11]	GG [16]
Rotation Attack (θ=10)	Barbara	**0.9968**	0.8596	0.9749	0.8172
	Airplane	**0.9971**	0.9025	0.8916	0.9227
	Boat	**0.9853**	0.8848	0.9770	0.7416
	Lena	**0.9806**	0.7498	0.8502	0.6681

V. CONCLUSION

A detector was proposed for multiplicative watermarking in the contourlet domain based on tLS distribution. Accordingly Neyman-Pearson criterion, the LRT is optimal for designing the watermark detector. So in this work, we used LRT test.

Performance of our watermark detector was examined based on several experiments and compared with additive tLS, BKF, and GG detectors in the contourlet domain. The results confirm that our watermarking detector was superior to other schemes. Besides, it provided high robustness against different attacks.

REFERENCES

[1] T. Zong, Y. Xiang, I. Natgunanathan, S. Guo, W. Zhou, and G. Beliakov,"Robust histogram shape-based method for image watermarking", *IEEE Transactions on Circuits and Systems for Video Technology*, vol. 20, no. 3, pp. 717-729, 2015.

[2] N. Kalantari, S. M. Ahadi, M. Vafadust, “A robust image watermarking in the ridgelet domain using universally optimum decoder,” IEEE Transactions on circuits and systems for video technology, vol. 20, pp. 396-406, Mar 2010.

[3] .I. J. Cox, J. Kilian, F. T. Leighton, and T. Shamoon, “Secure spread spectrum watermarking for multimedia,” *IEEE Trans. Image Process.*, vol. 6, no. 12, pp. 1673–1687, Dec. 1997.

[4] E. Nezhadarya, Z. J. Wang, and R. K. Ward, “Robust image watermarking based on multiscale gradient direction quantization”, *IEEE Transactions on Information Forensics and Security*, vol. 6, no. 4, pp. 1200-1213, 2011.

[5] L. Hsu, H. Hwai-Tsu, “Blind image watermarking via exploitation of inter-block prediction and visibility threshold in DCT domain,” Journal of Visual Communication and Image Representation, vol. 32, pp. 130-143, Oct 2015

[6] C. Hsieh, L. Chi-Jen, "A novel image watermarking scheme based on amplitude attack." Pattern Recognition, vol. 40, pp. 1342-1354, Apr 2007.

[7] V. R. Doncel, , N. Nikolaidis, I. Pitas, “An optimal detector structure for the Fourier descriptors domain watermarking of 2D vector graphics,” IEEE Transactions on Visualization and Computer Graphics, vol. 13, pp. 851-863, Jul 2007.

[8] M. Amirmazlaghani, M. Rezghi, H. Amindavar, “A novel robust scaling image watermarking scheme based on Gaussian Mixture Model,” Expert Systems with Applications, vol. 42, pp. 1960-1971, Mar 2015.

[9] M.Amirmazlaghani, “Additive watermark detection in the wavelet domain using 2D-GARCH model,” Information Sciences, vol. 370, pp. 1-17, Nov 2016.

[10] S. Etemad, M. Amirmazlaghani, “Additive watermark detector in contourlet domain using the t location-scale distribution,” 2nd International Conf. Signal Proc. and Intell. Sys., pp. 1-5, Dec 2016.

[11] M. Rabizadeh, M. Amirmazlaghani, M. Ahmadian-Attari, “A new detector for contourlet domain multiplicative image watermarking using Bessel K form distribution,” Journal of Visual Communication and Image Representation, vol. 40, pp. 324-334, Oct 2016.

[12] H. Sadreazami, M. Amini, “A robust spread spectrum based image watermarking in ridgelet domain,” AEU-International Journal of Electronics and Communications, vol. 66, pp. 364-371, May 2012.

[13] M. Do, M. Vetterli, “The contourlet transform: an efficient directional multiresolution image representation,” IEEE Transactions on image processing, vol. 14, pp. 2091-2106, Dec 2005.

[14] Q. Cheng and T. S. Huang, “Robust optimum detection of transform domain multiplicative watermarks,” *IEEE Transactions on Signal Processing,* vol. 51, no. 4, pp. 906-924, 2003.

[15] D. Po, M. Do, “Directional multiscale modeling of images using the contourlet transform,” IEEE Transaction on image processing, vol. 15, pp. 1610-1620, Jun 2006.

[16] M. Akhaee, S. Sahraeian, F. Marvasti, “Contourlet-based image watermarking using optimum detector in a noisy environment,” IEEE Transactions on Image Processing, vol. 19, pp. 967-980, Apr 2010.

[17] H. Sadreazami, M. Ahmad, M.S. Swamy, “Optimum multiplicative watermark detector in contourlet domain using the normal inverse Gaussian distribution,” IEEE international Symp. On Circuits and Sys, pp. 1050-1053, May 2015.

[18] H. Sadreazami, M. Ahmad, MN Swamy, “A study of multiplicative watermark detection in the contourlet domain using alpha-stable distributions,” IEEE Transactions on Image Processing, vol. 23, pp. 4348-4360, Oct 2014.

[19] S. Kotz, S. Nadarajah, “ Multivariate t-distributions and their applications”. Cambridge University Press, 2004.

[20] Online Image Database. *[Online]. Available: http://decsai.ugr.es/cvg/CG/base.html, accessed Mar. 2013.*